

Solid state intermetallic compound layer growth between copper and hot dipped indium coatings

P. T. VIANCO, A. C. KILGO, R. GRANT

Center for Solder Science and Technology, Sandia National Laboratories, Albuquerque, NM, USA

Solid state growth of intermetallic compound layers that form between hot dipped indium coatings and copper was investigated in diffusion couples aged at temperatures of 70, 100 and 135 °C and time periods of up to 300 days. At an annealing temperature of 70 °C, the metastable composition, $\text{Cu}_{36}\text{In}_{64}$, was observed at the interface. Ageing at 100 °C caused a dual layer structure with the $\text{Cu}_{36}\text{In}_{64}$ layer joined by a copper-rich intermetallic compound, $\text{Cu}_{11}\text{In}_9$, that is noted in the equilibrium phase diagram. An annealing temperature of 135 °C caused the eventual development of a single copper-rich intermetallic layer, $\text{Cu}_{57}\text{In}_{43}$, at the interface. Total intermetallic layer thickness was documented as a function of ageing time and temperature, exhibiting a $t^{1/2}$ dependence with an apparent activation energy of 20 kJ mol⁻¹.

1. Introduction

The assembly of electronic systems has relied heavily upon the use of tin-lead solders, e.g. 63 Sn–37 Pb or 60 Sn–40 Pb, wt %) for device attachment to the printed wiring boards or (hybrid) ceramic substrates. However, those applications which include cryogenic environments (satellites, spacecraft, etc.), step soldering sequences, or the assembly of heat sensitive devices may require lower melting temperature solders. In those cases, the indium-based solders, such as 52 In–48 Sn (eutectic temperature, $T_{\text{eutectic}} = 118^\circ\text{C}$) and 100 In (temperature of melting, $T_{\text{melt}} = 156^\circ\text{C}$), have found widespread use [1].

Functionally, solder joints must provide not only an electrical conduit for signal transmission, but also, with the advent of surface mount technology, serve as a mechanical fastener to secure the package to the circuit board. The manufacturability and service reliability of electronic products depend upon the integrity of the solder joints, which is determined by the microstructure of both the solder alloy as well as that of the solder–base metal interface.

The dissimilarity between solders and commonly used base metal such as copper, results in the development of reaction products at the solder–base metal interface. These reaction products are typically covalently bonded intermetallic compounds. For example, Cu_6Sn_5 and Cu_3Sn are the interface reaction layers formed between pure tin (and tin-based solders, such as 63 Sn–37 Pb) and copper (Fig. 1) [2, 3]; the latter layer appears only after extensive solid state thermal ageing. Intermetallic compounds tend to exhibit poor solderability after exposure to air, thereby affecting product manufacturability. In addition, their poor ductility can degrade the mechanical integrity of the solder joint, particularly when the circuit board is

exposed to high impact loading conditions. Intermetallic compound layers form while *molten* solder is in contact with the base metal during the assembly process. Moreover, the layer(s) continue to grow after solidification, through solid state diffusion processes. The rate of solid state growth depends upon the temperature conditions and time duration.

The interfacial chemistry which develops in the solder joint by solid state diffusion processes may exhibit one or more of the equilibrium phases denoted in the phase diagram, e.g. the tin–copper system noted above. It is conceivable that non-equilibrium or metastable phases may appear and disappear as a result of the diffusion processes responsible for development of the interfacial chemistry. Moreover, a previous study has shown that the thickness of the layer(s) can depend upon the physical metallurgy (composition or microstructure) of the solder coating [4].

The phase diagram of the indium–copper system appears in Fig. 2 [5]. Clearly, a number of line compounds exist between copper and indium under equilibrium conditions, depending upon the temperature and starting composition. Barnard investigated indium–copper diffusion couples fabricated by the electroplating of indium on the copper substrate [6]. A single line compound was observed at the indium–copper interface: $\text{Cu}_{11}\text{In}_9$. The growth kinetics were parabolic with an apparent activation energy of 24 kJ mol⁻¹. A similar finding was made by Manna *et al.* for indium–copper couples formed by vapour deposited indium films on single crystal copper substrates [7]. Once again, only the $\text{Cu}_{11}\text{In}_9$ layer was observed; it grew with an apparent activation energy of 26 kJ mol⁻¹. In each of these previous studies, the indium layer was applied at ambient temperatures as a solid coating so that interactions at the

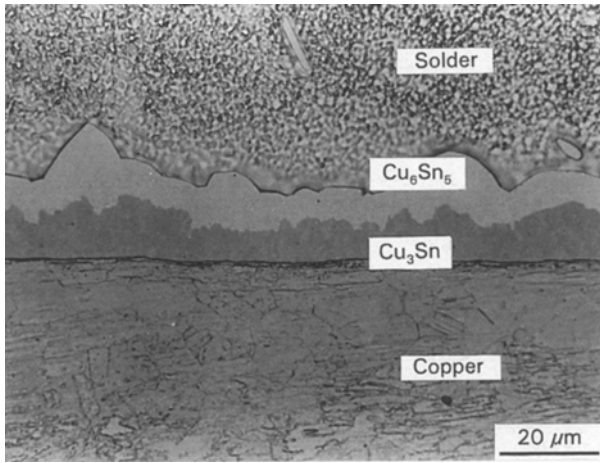


Figure 1 Optical micrograph of the Cu_6Sn_5 and Cu_3Sn intermetallic layers: the interface between pure tin and copper after thermal ageing at 170 °C for 200 days.

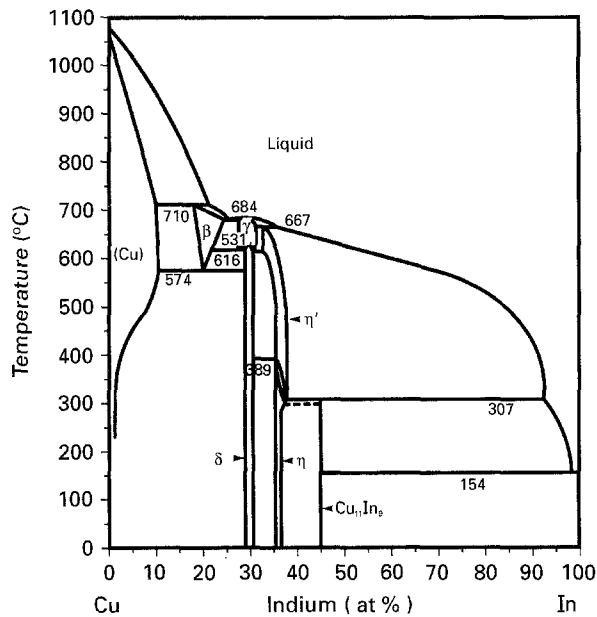


Figure 2 Cu–In binary phase diagram [5].

indium–copper interface were minimal prior to solid state ageing.

The present study examined intermetallic compound layer development between hot dipped pure indium coatings and copper through solid state thermal ageing. Hot dipped coatings are metal layers which are applied to the substrate surface by immersing the base metal into a bath of the molten solder, in this case, pure indium. These coatings are used widely as protective finishes on electronic package leads and terminations in order to protect their solderability from deterioration by contamination or excessive surface oxidation. The composition of the intermetallic layer was documented by an electron microprobe analysis of the indium–copper interface structure. Growth kinetics of the intermetallic layer were analysed by measuring layer thickness as a function of temperature and time.

2. Experimental procedure

2.1. Sample preparation

The substrates used in this investigation were oxygen-free, high conductivity (OFHC) copper tabs punched from sheet stock and measuring $0.635 \times 0.635 \times 0.159$ cm. The composition of the copper was verified by atomic emission spectroscopy to have contaminant levels less than the following values: 40 p.p.m. Ag, 50 p.p.m. Al, 10 p.p.m. Mg, 30 p.p.m. Mn and 10 p.p.m. Si. The surface from which the thickness values were measured, was optically polished. Each specimen was solvent degreased, coated with a water soluble flux, and then dipped into a bath of molten indium metal for 5 s. The melting temperature of indium is 157 °C; however, the solder bath temperature was maintained at 200 °C to assure adequate wetting. The copper tab was immersed with the optically polished surface parallel to the solder surface and facing downwards. This orientation caused a large accumulation of solder to form on the optically polished surface upon withdrawal of the specimen from the bath. Therefore, the diffusion couple was comprised of effectively infinite sources of both copper and indium which supported the interfacial reaction.

Thermal ageing of the solder-coated test samples was performed in air furnaces. The annealing temperatures were 70, 100 and 135 °C with a temperature stability of ± 0.5 °C. The annealing time periods were 1–300 days with a tracking error of ± 30 min. Upon completion of the ageing treatment, each specimen was cross-sectioned and prepared for metallographic analysis.

2.2. Sample analysis

Intermetallic layer thickness measurements were performed by quantitative image analysis. It was determined in a previous study that a minimum of 40 data points would be adequate for the analysis [4]. Ten thickness measurements were taken from $\times 1000$ images of four regions along the indium–copper interface. The minimum thickness value resolved by the technique was 0.5 μm . The data pertaining to each particular annealing time and temperature condition were represented by the mean and plus/minus one standard deviation about the mean.

Compositions of the intermetallic layers were determined by electron microprobe analysis (EMA). Line traces of the elemental concentrations were made perpendicular to the interface (Fig. 3). Concentration changes along the trace designated the boundaries of the intermetallic layers. A sample point midway between such changes was used to designate the composition for that particular layer. Ten such traces were made per test sample in order to establish the composition of the layer(s). The spatial resolution of the concentration profile was a radius of 1.5 μm about the target point. The samples selected for the electron microprobe analysis provided a matrix of the following time and temperature values from which to examine the

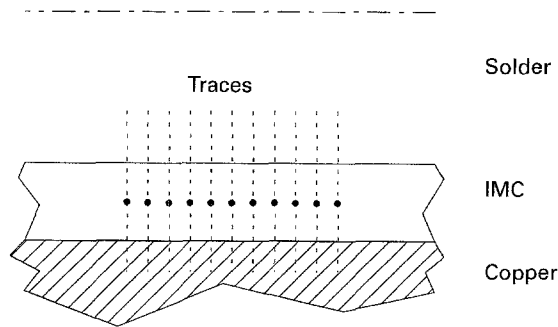


Figure 3 Line trace orientation for electron microprobe analysis of the intermetallic compound (IMC) layers.

development of the interfacial chemistry

70 °C; 2, 100, 200 days

100 °C; 2, 100, 200 days

135 °C; 2, 100, 200 days

3. Results and discussion

3.1. Interface compositional analysis

In the case of the as-fabricated specimens, the intermetallic compound layer thickness was $2.7 \pm 0.4 \mu\text{m}$; this value is relatively large as compared with initial thicknesses of 1–2 μm observed for tin-based solders on copper [4]. In similar experiments on the 50 In–50 Pb alloy, the as-fabricated intermetallic layer thickness was $3.16 \pm 0.94 \mu\text{m}$ which is also quite large [8]. Since the immersion temperature of the 50 In–50 Pb alloy was 10–30 °C below that of the tin-based solders, these data suggest that intermetallic layers developed from the indium-based solders have a faster formation rate than those created by the tin-based solders.

A spot analysis was performed on the as-formed intermetallic layer; the composition was determined to be $\text{Cu}_{44}\text{In}_{56}$ (at%) with a standard deviation of 6 at%. Scatter was attributed to the limited thickness of the layer as well as to apparent compositional variations in the layer itself.

An electron microprobe analysis of the intermetallic layer composition was performed on aged specimens as described earlier. An optical micrograph of the intermetallic layer which had developed in an indium–copper sample is shown in Fig. 4 for illustrative purposes. Samples aged at 70 °C for two days exhibited a single intermetallic layer (Fig. 5a). The composition of the layer was determined by the layer midpoint analysis (Fig. 5b) to be 63 ± 2 at% indium and 37 ± 2 at% copper, or $\text{Cu}_{37}\text{In}_{63}$. There were no significant changes in the layer composition after 100 or 200 days. However, several 200 day traces revealed a small cusp in the concentration values within the layer (Fig. 6). The cusp represented a region of decreased indium concentration and correspondingly, increased copper. The limited width of the region and its intermittent occurrence prevented further quantitative analyses.

Next, samples heat treated at 100 °C were examined. Following an annealing period of two days, the single intermetallic compound layer composition had

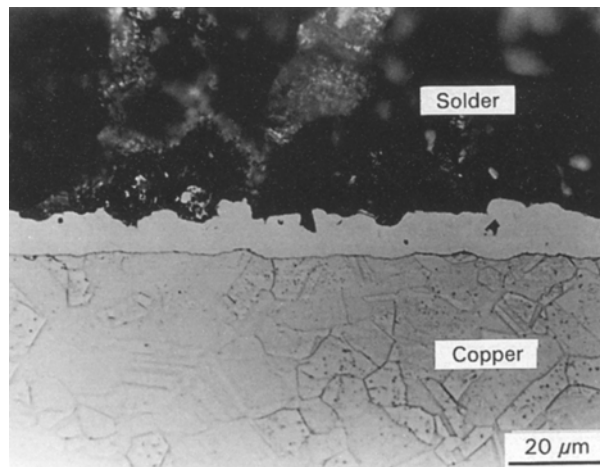


Figure 4 Optical micrograph of the intermetallic layer formed between pure indium and copper following thermal ageing at 100 °C for 350 days.

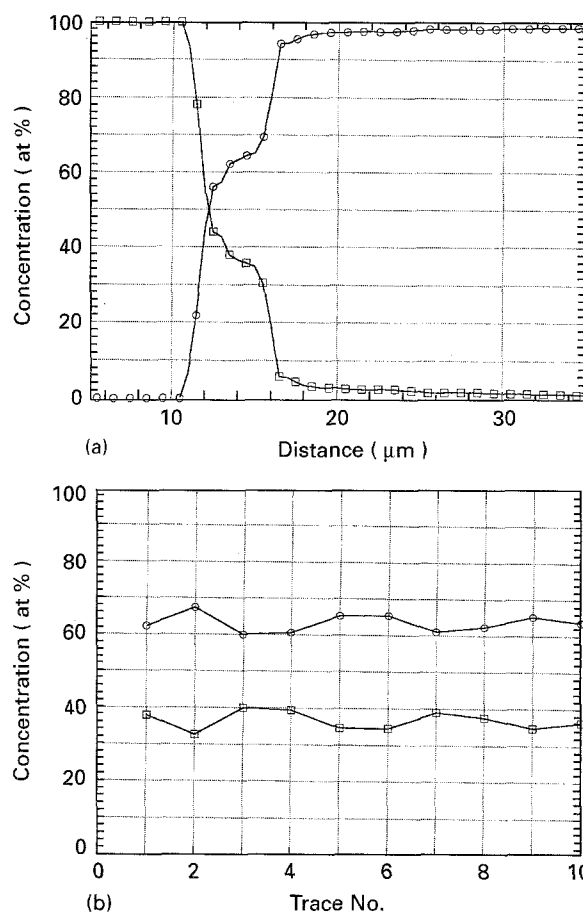


Figure 5 (a) Electron microprobe trace across the intermetallic layer of the indium–copper couple annealed at 70 °C for two days, and (b) midpoint composition trace for the intermetallic layer in the same sample: (–○–) indium, (–□–) copper.

a slightly reduced indium content of 60 ± 6 at% as compared with the corresponding value of 63 ± 2 at% for the 70 °C, two day data. Scatter in the elemental concentrations was significantly higher in the 100 °C results. Heat treatment for 100 days caused the development of a second, copper-rich intermetallic layer (Fig. 7) which was observed intermittently along the indium–intermetallic layer interface. The composition of the second layer had an apparent

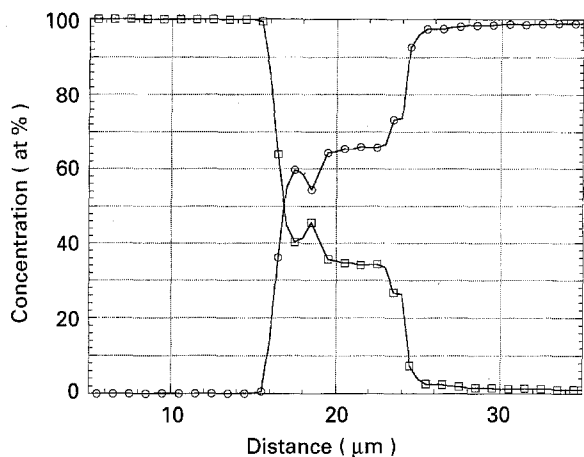


Figure 6 Electron microprobe trace across the intermetallic layer of the specimen annealed for 200 days at 70 °C: (—○—) indium, (—□—) copper.

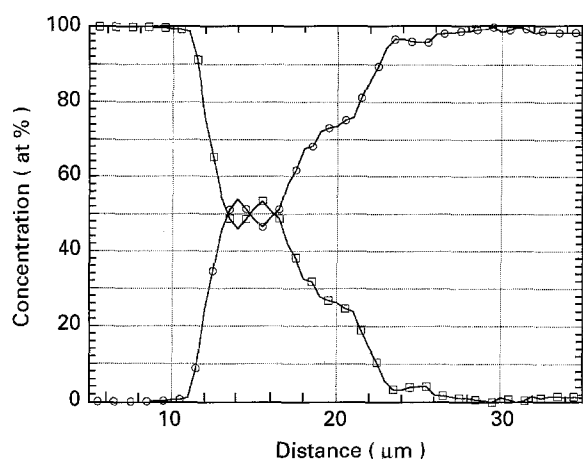


Figure 7 Electron microprobe trace across the intermetallic layer of the specimen annealed at 100 °C for 100 days: (—○—) indium, (—□—) copper.

stoichiometry of $\text{Cu}_{54}\text{In}_{46}$ (± 2 at %). In those regions with multiple layers, the indium-rich layer which was retained next to the copper substrate, had a composition of $\text{Cu}_{46}\text{In}_{54}$ (± 2 at %). For the most part, the interface microstructure was dominated by a single intermetallic layer with an indium content of 57 ± 4 at %, which was reduced in comparison to the 70 °C ageing specimens.

The appearance of the copper-rich intermetallic sublayer near the indium coating was somewhat unexpected. It would be anticipated that such a layer would develop next to the copper substrate in order to diminish the copper concentration gradient across that interface. However, simply the presence of the copper-rich layer as well as a slightly reduced indium content in the indium-rich layer suggest a reduction in the overall indium and copper concentration gradients across the indium–copper interface. It is uncertain as to whether the copper-rich layer formed by diffusion of the elements or were a result of partial transformation of the $\text{Cu}_{46}\text{In}_{54}$ layer that was already present.

Extending the 100 °C ageing treatment to 200 days caused the development of an interface structure with either single or multiple intermetallic layers as was

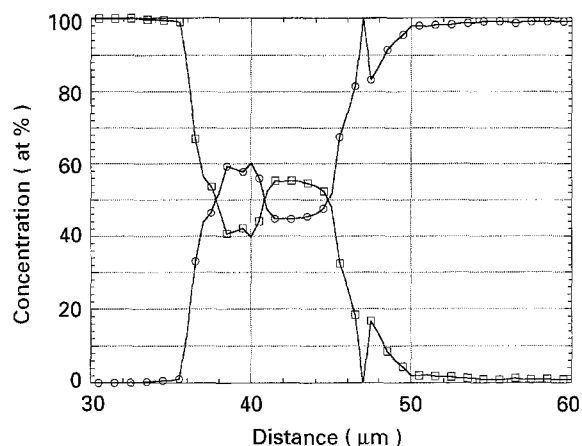


Figure 8 Electron microprobe trace across the intermetallic layer of the specimen annealed at 100 °C for 200 days: (—○—) indium, (—□—) copper.

similarly observed with the 100 day data. However, the dual layer structure (Fig. 8) was predominant, with the copper-rich layer thicker than its indium-rich counterpart in several observations. In addition, a small shelf in the copper trace developed at the copper–intermetallic layer interface which was not observed on the previous specimens. The layer next to the copper substrate remained indium-rich with a composition of $\text{Cu}_{41}\text{In}_{59}$ (± 2 at %). The copper-rich intermetallic layer had a stoichiometry of $\text{Cu}_{55}\text{In}_{45}$ (± 1 at %). In both cases, the compositions were similar to those noted after 100 days.

Clearly, the data taken from samples heat treated for various times at a temperature of 100 °C showed a transition in the intermetallic layer structure from a single, indium-rich layer to a dual layer structure comprised of an indium-rich layer next to the copper substrate and the development of a copper-rich intermetallic layer near the indium coating. In addition, the stoichiometry of the indium-rich layer appears able to exist over a range of compositions, exhibiting a trend of decreased indium content with the extent of ageing.

The composition of the intermetallic layers formed in samples thermally annealed at 135 °C were next investigated. The double layer structure was observed over a large part of the interface after two day heat treatment. [A few isolated areas of a single (indium-rich) layer were also recorded.] The composition of the indium-rich layer was $\text{Cu}_{43}\text{In}_{57}$ (± 2 at %), which is not significantly different from that observed in two layer structure after the 100 °C heat treatment. The copper-rich layer next to the indium coating had a composition of $\text{Cu}_{55}\text{In}_{45}$ (± 1 at %), which also duplicated that noted for the 100 °C data.

Ageing at 135 °C for 100 days brought about a significant change in the intermetallic structure. A copper-rich intermetallic layer with the previously observed composition, $\text{Cu}_{55}\text{In}_{45}$, had developed adjacent to the copper substrate (Fig. 9). Recall that a shelf in the copper trace was observed to have developed at that interface in the samples annealed at 100 °C for 200 days. Between the $\text{Cu}_{55}\text{In}_{45}$ layer and the indium coating was observed either an indium-rich layer ($\text{Cu}_{35}\text{In}_{65}$, ± 3 at %), or the absence of any additional layers, altogether. In a few traces, the remnants of

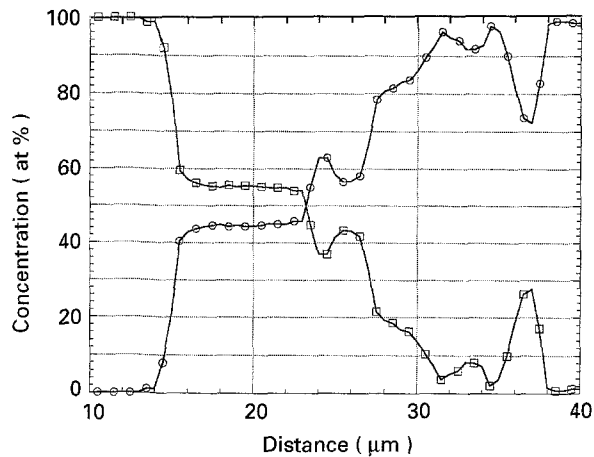


Figure 9 Electron microprobe trace across the intermetallic layer developed in the specimen annealed at 135 °C for 100 days: (—○—) indium, (—□—) copper.

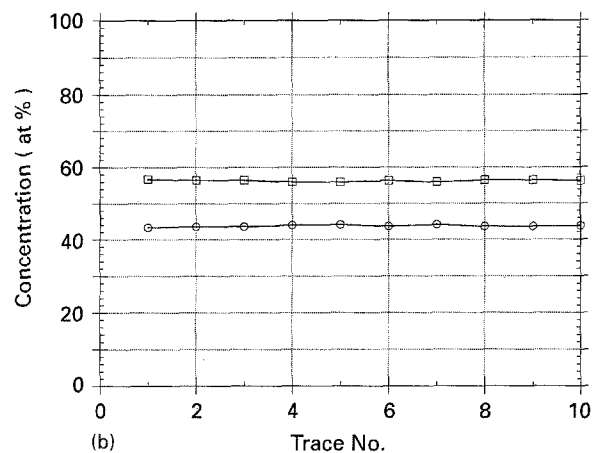
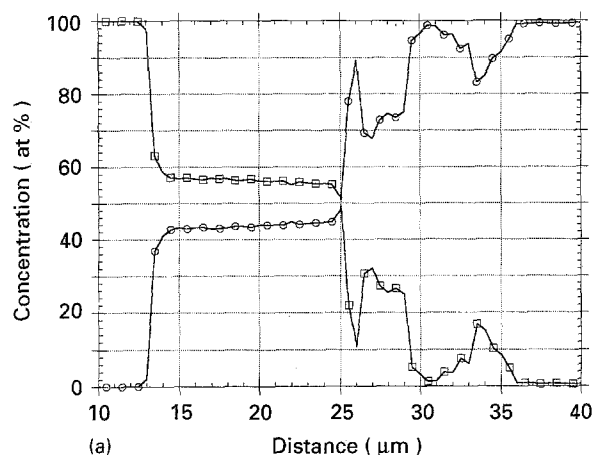


Figure 10 (a) Electron microprobe trace of the intermetallic layer in a sample aged at 135 °C for 200 days, and (b) centreline map of the ten traces across the intermetallic compound layer: (—○—) indium, (—□—) copper.

a copper-rich intermetallic layer were observed between the indium-rich intermetallic compound and the indium coating.

Finally, thermal annealing for 200 days (135 °C) established fully the development of a single intermetallic layer (Fig. 10a). The composition of the intermetallic layer was determined to be $\text{Cu}_{57}\text{In}_{43}$ (Fig. 10b) and was very similar to that of the copper-rich layers observed at lower annealing temperatures and/or shorter time periods.

The traces in Fig. 10 along, with that in Fig. 9, also show the presence of a gradual (albeit, not necessarily monotonic) decrease in the copper concentration as the profile progresses from the intermetallic layer boundary into the indium field. At lower ageing temperatures and shorter times, this transition was considerably more abrupt (Figs 5a and 6). The non-monotonic nature of the transition indicates that the change in copper or indium concentration was accomplished by regions (or “pseudo-compounds”) of varying copper and indium concentrations. The phase diagram indicates negligible solid solubility of either copper or indium in each other at these temperatures.

The electron microprobe data developed from thermal ageing at 70, 100 and 135 °C clearly demonstrate an evolution in the interface composition and layer microstructure. Using the 200 day data as a benchmark, the intermetallic compounds observed at temperatures of 70, 100 and 135 °C were

1. $\text{Cu}_{36}\text{In}_{64}$,
2. $\text{Cu}_{41}\text{In}_{59}$ + $\text{Cu}_{55}\text{In}_{45}$, and
3. $\text{Cu}_{57}\text{In}_{43}$, respectively.

The indium-rich intermetallic layer was generated between copper and the molten indium coating during the hot dipping process. At an ageing temperature of 70 °C, the layer had an indium concentration of 63–65 at % and continued to thicken with time. Heat treatments at 100 °C caused the development of the dual layer configuration with emergence of a copper-rich layer next to the indium field. A slight decrease in the indium content of the retained indium-rich layer was also noted. Solid state ageing at 135 °C resulted in the elimination of the dual layer structure in favour of the single, copper-rich intermetallic layer, $\text{Cu}_{57}\text{In}_{43}$. The transformation of the intermetallic structure by solid state diffusion suggests that the copper–indium interface was changing from the indium-rich structure characteristic of the molten indium–copper equilibrium, to a copper-rich configuration representative of the solid state equilibrium. This transition (together with the gradual change of copper content in the near-interface region of the indium field under harsher ageing conditions) resulted in an overall reduction in the copper and indium concentration gradients across the interface region.

The intermetallic layer compositions described above were compared to those recorded in the equilibrium phase diagram (Fig. 2) [5]. The $\text{Cu}_{36}\text{In}_{64}$ and $\text{Cu}_{41}\text{In}_{59}$ intermetallic layers were metastable compounds which do not appear in the phase diagram. In fact, the two compounds may simply be stoichiometric variations of the same structure. The metastable compositions appear to represent a product of conditions during the hot dipping procedure. The intermetallic layers, $\text{Cu}_{55}\text{In}_{45}$ and $\text{Cu}_{57}\text{In}_{43}$ are, to within experimental error, the same stoichiometry as the $\text{Cu}_{11}\text{In}_9$ composition found in the phase diagram (see Fig. 2). As noted earlier, the $\text{Cu}_{11}\text{In}_9$ layer was observed as the interface composition of copper–indium couples in the ageing experiments conducted by other investigators [6, 7].

These observations suggest the following generalization pertinent to the ageing of solder joint interfaces.

The equilibrium interfacial chemistries can differ between the liquid solder–substrate and solidified solder–substrate conditions. As a result, solid state ageing of diffusion couples formed by the hot dipped application of the solder coating may involve complex compositional changes as well as general thickening of the intermetallic layer as the system develops phases characteristic of the solid state equilibrium (represented by the traditional phase diagram).

3.2. Intermetallic compound layer growth kinetics

The total thickness of the intermetallic layer as a function of the square root of time (up to 300 days) for the various ageing temperatures is shown in Fig. 11. From the electron microprobe data described above, the curve at 70 °C largely represented growth of the indium-rich $\text{Cu}_{36}\text{In}_{64}$ layer. At 100 °C, thickness values for two days were also pertinent to the indium-rich layer; however, at longer time durations, the thickness data represented combined growth of both the indium- and copper-rich layers. When the multiple layers were present, data measurements of the individual layers were not pursued due to their intermittent nature and variable relative thickness. The data at 135 °C describe growth of the combined indium-rich and copper-rich sublayers at the shorter time periods of up to 100 days. For durations of 200 days and longer, thickness values described growth of solely the $\text{Cu}_{57}\text{In}_{43}$ layer.

Regression analysis revealed that the data was best fit with a parabolic time dependence as shown in the plot. The $t^{1/2}$ behaviour suggests that the rate controlling mechanism for layer growth was largely volume diffusion [9]. Fluctuations in the intermetallic layer thicknesses increased with longer ageing times and higher ageing temperatures.

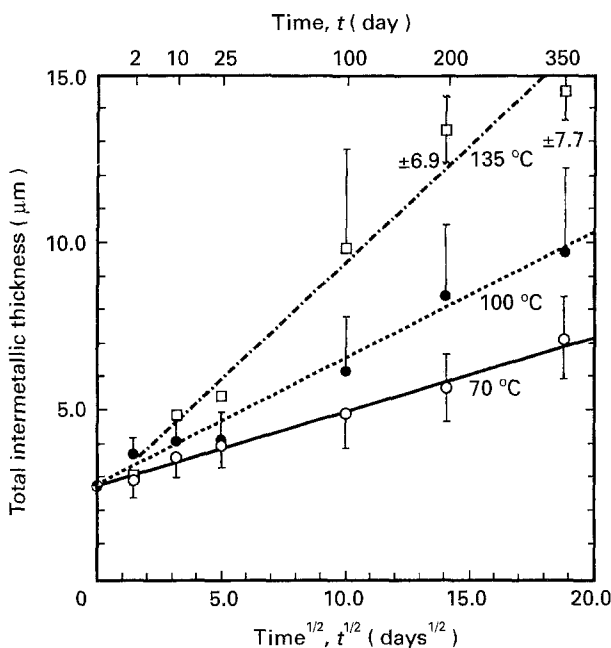


Figure 11 Total intermetallic thickness as a function of the square root of time for the indium–copper couples.

A comparison was made between the data for the indium–copper system in Fig. 11 with that of the more familiar tin–copper system in Fig. 12 [4]. At 70 and 100 °C, the indium–copper system produced thicker layers as compared with the tin–copper system. This result was due to both a thicker initial layer as well as a faster growth rate in the indium–copper system. At 135 °C, the intermetallic layer thicknesses for the two systems were comparable, due in large part to a slightly greater growth rate for the tin–copper system.

An apparent activation energy analysis was performed on the growth data. The experimentally measured property upon which the Arrhenius plot was developed, was the growth rate of the intermetallic layer. Since the diffusion of a single atomic species (Cu or In) could not be identified as rate controlling, the apparent activation energy did not represent the activity of any one specific atomic process. It was assumed that the intermetallic layer thickness was represented by the empirical relation

$$y(t) = y_0 + At^n \exp(-Q/RT) \quad (1)$$

where $y(t)$ is the layer thickness at time, t ; y_0 is the initial thickness; A is a numerical constant; n is the time exponent; Q is the apparent activation energy; T is the temperature; and R is the universal gas constant. The apparent activation energy was computed from the logarithm-differential of Equation 1

$$d[\ln(dy/dt)]/d(1/T) = -Q/R \quad (2)$$

The plot of $\ln(dy/dt)$ as a function of $1/T$ (at $t = 100$ days) is shown in Fig. 13; the apparent activation energy, Q , was calculated by a linear regression analysis of the data and determined to be 20 kJ mol^{-1} .

Recall that earlier solid state ageing studies performed by Barnard [6] and Manna *et al.* [7] for indium coatings on copper resulted in similar apparent activation energies of 24 and 26 kJ mol^{-1} , respectively. A comparison of these values with that of the

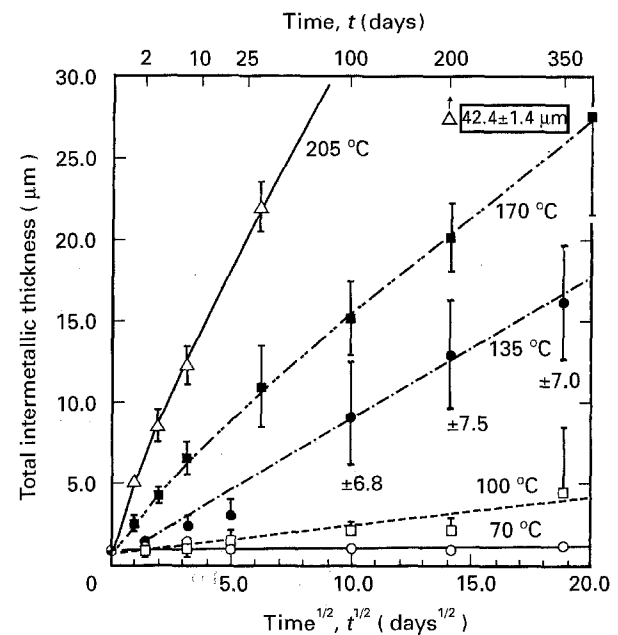


Figure 12 Total intermetallic thickness as a function of the square root of time for the tin–copper couples.

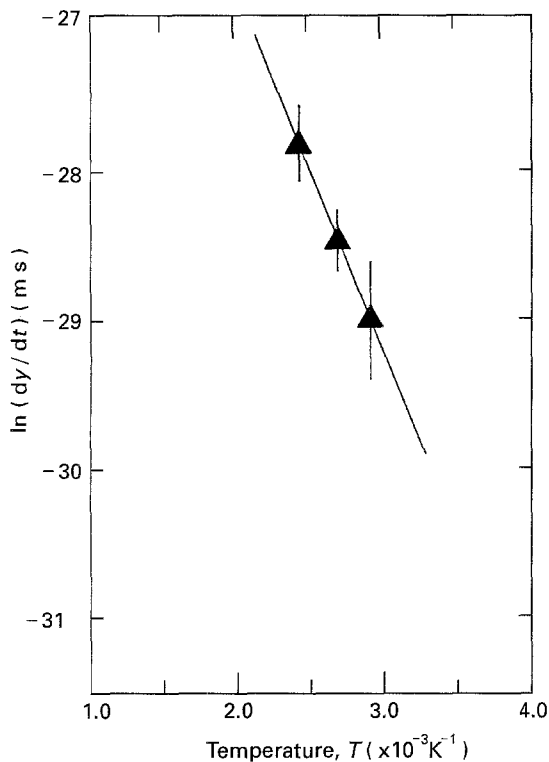


Figure 13 Apparent activation energy analysis of aged indium–copper samples, where $Q = 20 \text{ kJ mol}^{-1}$.

present study illustrates two points. First, similar apparent activation energies were observed in spite of different initial indium coating deposition morphologies, i.e. electrodeposited, vapour deposited or hot dipped. This observation suggests that the elevated temperature conditions accompanying the thermal ageing process assimilated the different microstructures, thereby negating any role played by the starting indium morphology (which characterized the particular deposition process).

A second point is that the different intermetallic layer compositions did not significantly impact the growth kinetics. For example, the electroplated or evaporated coatings would have a negligible as-deposited intermetallic layer thickness as compared with a $3.7 \mu\text{m}$ layer observed with the hot dipped samples. In addition, the hot dipped samples progressed through a series of intermetallic layer compositions as the ageing temperature and time increased. The metastable indium-rich layers appeared to exhibit a range of stoichiometries. The studies in [6] and [7] noted only a single layer composition, $\text{Cu}_{11}\text{In}_9$. Since the variable layer composition of the hot dipped coatings did not alter the apparent activation energy with respect to the single layer composition in the deposited coatings [6, 7], it would appear that the same volume diffusion mechanism was rate controlling in both the deposited and hot dipped films; the reaction processes responsible for the changing layer composition were not significant factors in the growth kinetics.

Finally, the apparent activation energy of intermetallic layer growth in hot dipped indium–copper couples (20 kJ mol^{-1}) is compared with data from hot dipped tin–copper couples [4]. In the latter case, the apparent activation energy value was 66 kJ mol^{-1}

when thickness data at 70, 100, 135, 170 and 205°C were included in the analysis. However, a knee in the Arrhenius plot of $\ln(dy/dt)$ versus $1/T$ (where y is the thickness, t is time and T is temperature) was observed at approximately 135°C . When the curve was split and an activation energy analysis was performed on the high temperature segment, i.e. 135, 170 and 205°C , a value of 25 kJ mol^{-1} was calculated, which is very similar to that for the indium–copper system.

The similarity of activation energies was examined with respect to the homologous temperatures represented by the ageing conditions. The homologous temperatures represented by 70, 100 and 135°C for the indium coating were nearly identical to those represented by the respective ageing temperatures of 135, 170 and 205°C for the case of tin. This comparison suggests that the growth processes for the indium–copper and tin–copper systems have similar kinetics at an equivalent homologous temperature. On the other hand, the growth rates of the intermetallic layer(s) in the tin–copper system were three to four times greater than those calculated for the indium–copper system (at the equivalent homologous temperature). This difference reflects the additional role that non-rate controlling factors (which are represented by the pre-exponential term of the Arrhenius plot) have on the intermetallic layer growth.

4. Conclusions

1. The development of the intermetallic compound layer formed at the interface between hot dipped indium coatings and copper by means of solid state thermal ageing, was investigated. The diffusion couples were heat treated at temperatures of 70, 100 and 135°C and for time periods of up to 300 days.

2. Electron microprobe techniques showed that the composition of the intermetallic layer changed with extent of ageing. An indium-rich layer ($\text{Cu}_{36}\text{In}_{64}$) was present for annealing terms of two through 200 days at a temperature of 70°C . The composition appeared to be metastable, since it was not observed in the equilibrium copper–indium phase diagram. For an ageing temperature of 100°C , the single layer ($\text{Cu}_{36}\text{In}_{64}$) was joined by the copper-rich $\text{Cu}_{11}\text{In}_9$ compound layer that is noted in the equilibrium phase diagram. Raising the ageing temperature to 135°C caused the dual layer structure to transform into a single, copper-rich intermetallic layer.

3. Growth of the total intermetallic layer thickness as a function of time and temperature was quantified. The thickness values exhibited a $t^{1/2}$ dependence by linear regression analysis, with an apparent activation energy of 20 kJ mol^{-1} .

4. The activation energy was similar to that calculated by previous investigators for electrodeposited indium coatings and vapour deposited indium thin films on copper. This comparison suggests that the growth kinetics of the intermetallic layer were not sensitive to the initial microstructure of the indium coating (electrodeposited, vapour deposited or hot dipped) nor to the presence of single or multiple layer compositions. Also, similar growth kinetics described

the tin-copper system when a comparison was made at equivalent homologous temperatures.

References

1. K. SEELIG, D. SKLARSKI, L. JOHNSON, and J. SARTTELL, in Proceedings, NEPCON East, June, 1987.
2. "Binary Alloy Phase Diagrams", edited by T. Massalski (American Society for Metals, Materials Park, OH, 1986) p. 965.
3. L. ZAKRAYSEK, *Weld J.* **51** (1972) 536s.
4. P. VIANCO, P. HLAVA and A. KILGO, *J. Elect. Mater.* **23** (1994) 583.
5. C. KAO, A. BOLCAVAGE, S. CHEN, S. CHEN, Y. CHANG and A. ROMIG, *J. Phase Equilibria* **14** (1993) 14.
6. R. BARNARD, *Plating* **61** (1974) 752.
7. I. MANNA, S. BADER, W. GUST and B. PREDEL, *Phys. Status Solidi* **119** (1990) k9.
8. D. FREAR and P. VIANCO, *Metall. Trans. A* **25** (1994) 1509.
9. E. MACHLIN, "An Introduction to Aspects of Thermodynamics and Kinetics", (Giro Press, Croton-on-Hudson, NY, 1991) pp. 190-193.

Received 29 September 1994

and accepted 11 April 1995